Reinforcement of Natural Rubber

LILIANE BOKOBZA, AND OLIVIER RAPOPORT

Laboratoire PCSM, E.S.P.C.I., 10 rue Vauquelin, 75231 Paris Cedex, France

Received 22 June 2001; accepted 11 December 2001

ABSTRACT: In this article, we report on recent investigations on filled natural rubber. These investigations include a mechanical characterization as well as a molecular analysis based on measurements of chain orientation. It is demonstrated that at intermediate strains, the increase in the moduli can be explained by the inclusion of rigid particles in the soft matrix and from molecular interactions between the rubber and the filler. These interactions can be evaluated by equilibrium swelling and by orientational measurements. With regard to the unfilled formulation, carbon black– and silanized-filled natural rubber exhibit increases in the cross-linking density ascribed to filler-polymer links, whereas a large decrease in the orientational level, evidenced by birefringence and by infrared dichroism, is observed when silica is added without any coupling agent. Finally, two specific effects—the Payne and Mullins effects, both related to energy dissipation phenomena—are discussed. © 2002 Wiley Periodicals, Inc. J Appl Polym Sci 85: 2301–2316, 2002

Key words: elastomers; reinforcement; fillers; mechanical properties; orientation; natural rubber

INTRODUCTION

A wide variety of particulate fillers are used in the rubber industry to improve and modify the physical properties of elastomeric materials. The addition of filler usually leads to increases in modulus and to significant improvements in abrasion and tear resistance.

Although the mechanisms of reinforcement are not fully understood, there is a general agreement about the basic processes contributing to the stress–strain behavior of filled vulcanizates.[1–7] In addition to the expected increase in the modulus resulting from the inclusion of rigid filler particles in the soft matrix, another contribution arises from filler–rubber interactions, leading to additional cross links into the network structure. The behavior at large strains is governed by the limited chain extensibility reached by strain-amplification effects. The short chains connecting filler particles will experience different overstrains, which will depend on their local filler concentration. Stress softening is attributed to the breaking or slipping, from the particle surface, of chains attaining their limit of extensibility. Another consequence of the incorporation of filler in an elastomer is the significant change in the dynamic properties of the rubber. This phenomenon, of great importance in the rubber industry, attracted a great deal of interest. Filler networking, formed by filler–filler interactions or via a model of immobilized elastomeric layers on the filler surface, seem to be one of the main parameters that governs the dynamic response.

Filler morphology such as particule size, structure, and, essentially, surface characteristics have a large influence on the physical performance of the elastomeric material. Most important, however, are the surface characteristics and the chemically active sites, which determine the interaction between the filler and the polymer chains. This interaction is the key parameter in

Correspondence to: L. Bokobza (liliane.bokobza@espci.fr).

Journal of Applied Polymer Science, Vol. 85, 2301–2316 (2002)

Table I. Formulations of the rubber compounds.

Ingredients (phr)	NR1	NR2	NR3	NR4
Natural rubber	100	100	100	100
Cyclohexyl benzothiazole sulfenamide (CBS)	1.5	1.5	1.5	1.5
Stearic acid	2	2	2	2
Zinc oxide	3	3	3	3
Sulfur	1.5	1.5	1.5	1.5
Silica ($125 m^2/g$)	0	50	50	0
Si69	0	0	4	0
Carbon black	0	0	0	50

rubber reinforcement, and a better characterization of this interfacial interaction is essential for understanding the mechanism of rubber reinforcement. Such interaction which leads to an adsorption of the network chains onto the particle surfaces, can result from physical interaction arising from Van der Waals forces between the surface and the polymer or from chemical interaction, which can be met directly by chemisorption of elastomer on active sites or indirectly by means of coupling agents used in the case of a filler having poor adhesive qualities for a polymer. Coupling agents are generally bifunctional molecules that are able to establish molecular bridges at the interface between the polymer matrix and the filler surface, as in the case of a silica-filled hydrocarbon rubber.[1] The rubber–filler adhesion is increased and, as a consequence, the reinforcing capability of silica is enhanced. One of the most effective coupling agents for sulfur-cured compounds filled with nonblack fillers is mercaptopropyltrimethoxysilane (Dynasilan). The bis(3-triethoxysilylpropyl)tetrasulfide (TESPT), commonly abbreviated Si69, has widened the use of silica in rubber applications. It is often mentioned that the tetrasulfane function of the Si69 reacts with the polymer under curing conditions, thus leading to an additional network cross linking, rather than to interfacial coupling.[8,9]

A lot of work has been devoted to a combined investigation of carbon blacks, silicas, and organosilanes. Despite considerable research and development efforts to elucidate their action in the reinforcement process, new insights can be gained through recent investigations carried out with state-of-the-art techniques: infrared dichroism and birefringence, which are able to gather information at a molecular level.[10]

This article describes investigations carried out on filled natural rubber. In addition to mechanical and swelling measurements, Fourier transform infrared (FTIR) dichroism and birefringence are used to analyze the orientational properties of the networks filled with a nonblack filler such as silica.

EXPERIMENTAL PART

Samples

All the samples contain a fixed content of natural rubber (100 phr) and an identical amount of accelerator and sulfur and are, thus, expected to lead to a series of materials of the same chemical cross-linking density. One sample was prepared without the addition of a filler; the others contain carbon black (N 330 from Degussa (Ambès, France); surface area of about 83 m^2/g) or silica (Ultrasil VN 2 from Degussa (Wesseling, Germany); surface area of 125 m^2/g). Among the samples filled with silica, one was compounded with the Si69 coupling agent.

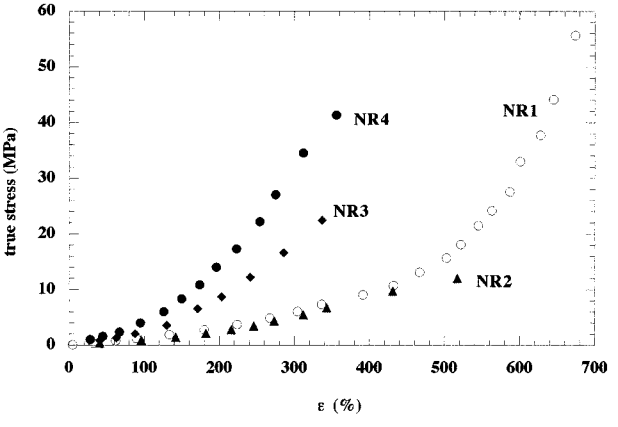

Figure 1 Stress–strain curves of the samples investigated.

Table II. Equilibrium swelling ratios, apparent molecular weight between cross-links, M_c, and orientational characteristics.

Sample	NR1	NR2	NR3	NR4
Q	4.93	6.24	3.56	2.97
Qrubber	4.93	7.33	4.09	3.42
Apparent M_c* (g. mol^{-1}	4700	11350	3050	1950
10^5 Δn_{rubber} (birefringence)	84.7	40.4	133.2	—
10^4 D_0 (infrared dichroism)	15.2	8.3	22.6	—

* Determined by the swelling measurements (eq.3) by taking an interaction parameter χ equal to 0.43.

The mixtures provided by Formix (Orléans, France) were cured into plaques at 170°C during 15 minutes under pressure that was adjusted to get the required thichnesses.

The formulation and the vulcanization characteristics of the samples are compiled in Table I.

Methods of Investigation

The stress–strain measurements reported here were taken by simply stretching film strips of 40 $\times$ 10 $\times$ 0.5 mm^3 between two clamps by means of a sequence of increasing weights attached to the lower clamp. The distance between two marks was measured with a cathetometer after allowing sufficient time for equilibration.

To determine the equilibrium swelling of the vulcanizate, a sample of 20 $\times$ 10 $\times$ 2 mm was put into toluene. After 72 hours at room temperature, the sample was taken out of the liquid, the toluene removed from the surface, and the weight determined. The weight swelling ratio, Q, was also determined from the lengths of the sample in the unswollen and swollen states.

Infrared spectra were recorded with an FTIR spectrometer (Nicolet Model 210) with a resolution of 4 cm^{-1} and an accumulation of 32 scans.

Birefringence was measured by using an Olympus BHA polarizing microscope fitted with a Berek compensator.

The thickness of the films was measured with a micrometer comparator and averaged all along the specimen.

The dynamic properties of the vulcanizates were measured by means of a Rheometric Dynamic Analyser (Rheometrics RDA II, Champs-sur-Marne, France) at 1 Hz sinusoidal oscillation, using disc specimens with thicknesses of 2 mm diameters of 8 mm, operated in a shear mode.

RESULTS AND DISCUSSION

Stress–Strain Curves

Comparative stress–strain curves are shown in Figure 1. It is obvious that the addition of silica alone does not lead to a significant change in the stress–strain properties; a slight decrease in stress is observed in the low-deformation range and becomes more pronounced at higher strains. Large increases in the moduli are observed when

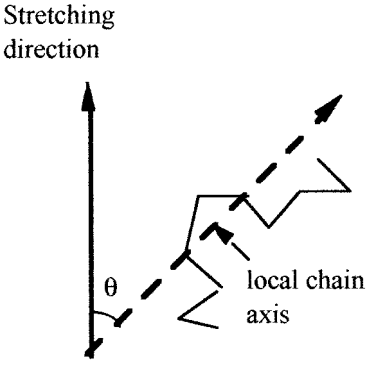

Figure 2 Definition of chain orientation.

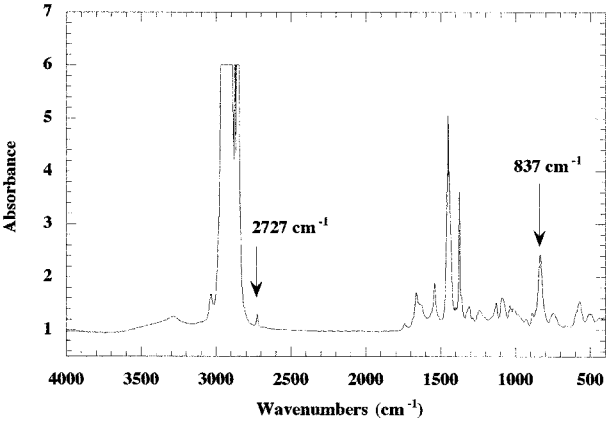

Figure 3 Midinfrared spectrum of natural rubber.

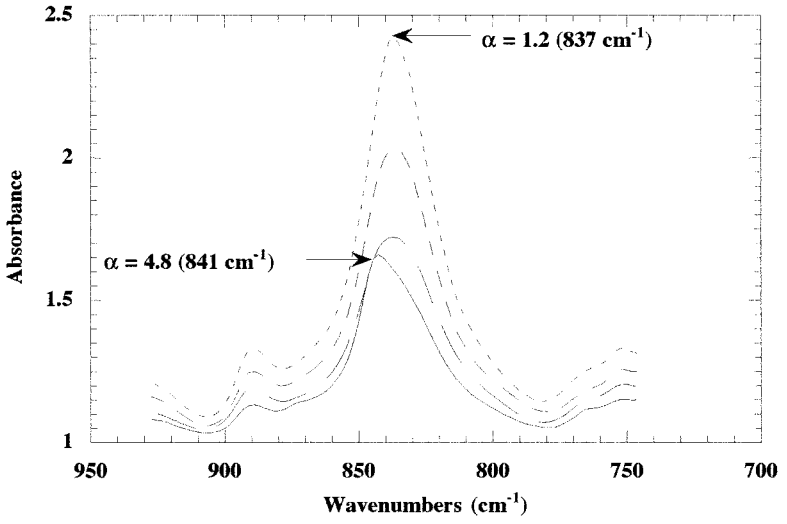

Figure 4 Shift of the out-of-plane absorption band on stress-induced crystallization.

natural rubber is filled with carbon black or with silica compounded with a coupling agent. As already known, the silanization of silica leads to fundamental changes in its reinforcing characteristics. However, silica is well known to affect the cross-linking density in vulcanization systems based on accelerator/sulfur cure systems.[11] The aim of this article is to quantify these effects.

The increase in stiffness imparted by an active filler is reasonably well understood. It involves a hydrodynamic effect arising from the inclusion of rigid particles and an increase in the cross-linking density created by polymer–filler bonding. In the absence of polymer–filler interaction, only hydrodynamic reinforcement is expected (sample NR2).

The inclusion of rigid filler particles is quantitatively taken into account by the Guth and Gold equation[12,13] given by this expression:

$$G = G_0 (1 + 2.5\varphi + 14.1\varphi^2) = G_0 X, \qquad (1)$$

where G_0 is the modulus of the matrix and φ is the volume fraction of filler.

This equation is based on Einstein's equation for the viscosity of a suspension of spherical rigid particles:[14]

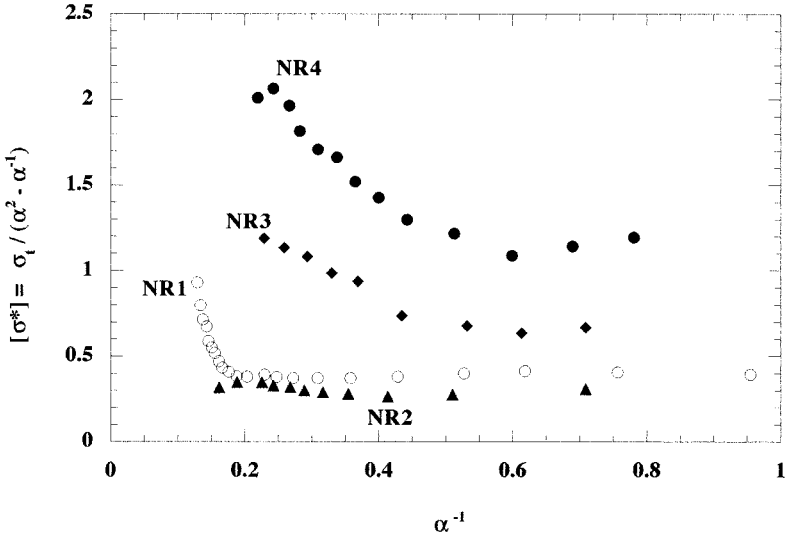

Figure 5 Mooney-Rivlin plots.

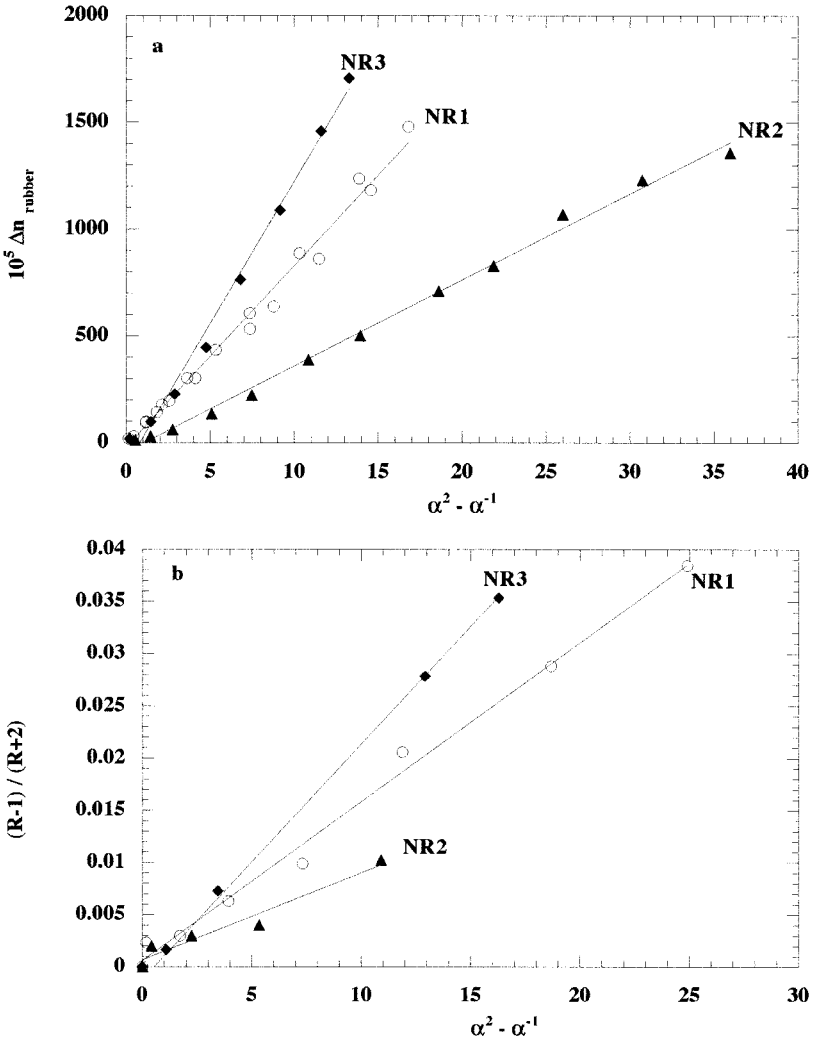

Figure 6 Orientation of polymer chains. (a) Birefringence; (b) infrared dichroism.

$$\eta = \eta_0 (1 + 2.5\varphi), \tag{2}$$

where η and η_0 are the viscosities of the suspension and the matrix, respectively.

Guth and Gold generalized the Einstein concept by adding the quadratic term to account for interaction between particles.

Equilibrium-Swelling Measurements

The other contribution to the reinforcement effect arises from molecular interaction between the rubber and the filler. This interaction leads to an increase in the effective degree of cross linking and can be evaluated by equilibrium swelling and by measurements of chain orientation.

The equilibrium-swelling analysis of elastomer vulcanizates is known to indicate the number of effective network chains per unit volume of rubber. For a filled vulcanizate, it should reflect not only the effects of chemical junctions but also the density of polymer–filler attachments.

The total network density can be estimated by the apparent molecular weight between cross links, M_c, given by the Flory–Erman equation:[15,16]

$$M_c = -\frac{\rho(1 - 2/\phi)V_1 v_{2m}^{1/3}}{\ln(1 - v_{2m}) + \chi v_2^{2m} + v_{2m}}, \tag{3}$$

where ρ denotes the network density during formation, V_1 is the molar volume of solvent, v_{2m} is the volume fraction of polymer at conditions of equilibrium, χ is the interaction parameter for the solvent–polymer system, and ϕ is the junction functionality.

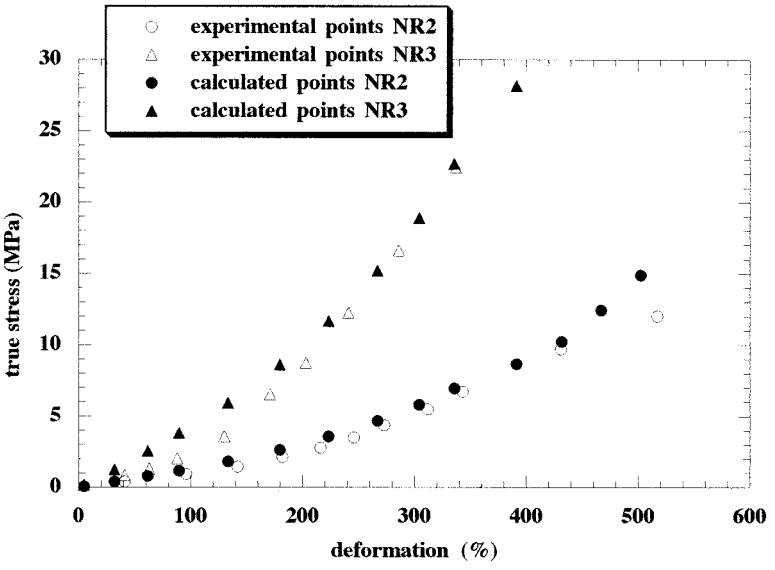

Figure 7 Experimental and calculated stress–strain curves for the NR2 and NR3 samples.

Under the assumption that the filler does not swell, we can calculate the equilibrium swelling ratio of the rubber alone, which is equal to

$$Q_{\text{rubber}} = \frac{Q - \varphi}{1 - \varphi}, \tag{4}$$

where φ is the volume fraction of filler.

As seen in Table I, the equilibrium swelling ratios decrease in carbon-black- and silanized-filled natural rubber with regard to the unfilled formulation, which reflects an increase in the cross-linking density ascribed to filler–polymer links. Conversely, the rubber swelling ratio increases substantially when silica is added without Si69. This result is attributed to the fact that silica affects the cross-linking density by reacting with the chemical ingredients of formulation, thus leading to a lower overall cure state.

Measurements of Chain Orientation

The analysis of the orientational behavior of filled networks, only applicable to systems filled with a nonblack filler, can provide a direct estimation of the total network chain density.

If a network is submitted to a uniaxial deformation, the polymer chains tend to orient along the direction of stretch. The orientation of segments under strain may be conveniently described by the second Legendre polynomial:[17]

$$\langle P_2 (\cos \theta)\rangle = \frac{1}{2} (3 \langle cos^2\theta\rangle - 1), \tag{5}$$

where θ is the angle between the macroscopic reference axis (usually taken as the direction of strain) and the local chain axis of the polymer (Fig. 2). The angular brackets indicate an average over all molecular chains and over all possible configurations of these chains.

The second moment of the orientation function $<P_2(\cos\theta)$ defined by eq. (1) may be related to network parameters and to the state of deformation by a series expansion[18–20] whose first term is

$$\langle P_2(\cos\theta)\rangle = D_0(\alpha^2 - \alpha^{-1}), \tag{6}$$

where D_0 is the configurational factor that depends on the choice of the molecular model of the network chain. In the first approximation, $\langle P_2(\cos\theta)\rangle$ is expressed as the product of a front factor, D_0, which incorporates the structural features of the network chains, and the strain function $(\alpha^2 - \alpha^{-1})$, which reflects the effect of the macroscopic deformation on orientation. α is the extension ratio, defined as the ratio of the final length of the sample in the direction of stretch to that of the initial length before deformation. The D_0 factor, which only reflects the "orientability" of the chain segments, is inversely proportional to the number n of bonds in the chain between two

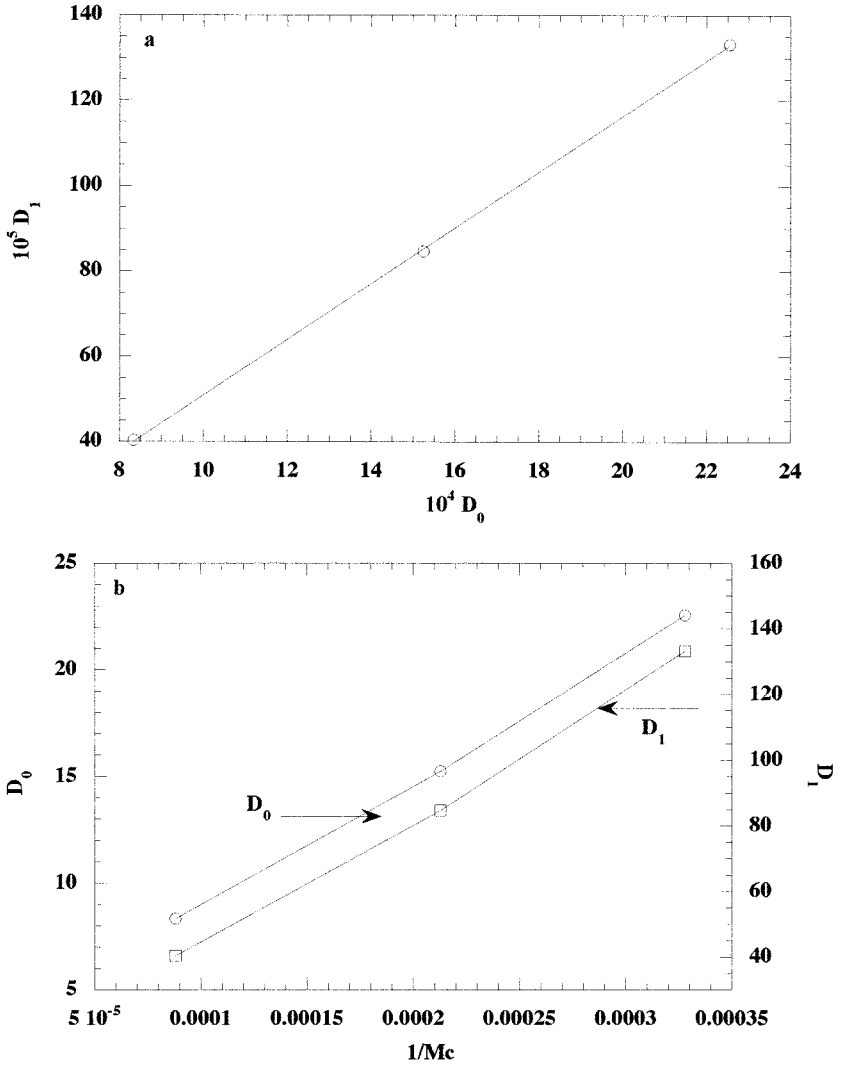

Figure 8 Relation between D_1 and D_0 (a) and dependence of D_0 and D_1 on the molecular weight betwen cross links, M_c (b).

junctions.[20] It can be evaluated from the rotational isomeric state formalism by using a Monte Carlo chain generation technique.

Eq. (6) holds for the orientation in a network chain exhibiting affine behavior. In the other extreme case of phantomlike chains, the expression for the orientation function becomes

$$\langle P_2(\cos\theta)\rangle = D_0\,(1 - 2/\phi)\,(\alpha^2 - \alpha^{-1}), \qquad (7)$$

The junctions' points are assumed to be embedded in the network and to transform affinely with macroscopic deformation in an affine network, while they are allowed to fluctuate over time without being hindered by the presence of the neighboring chains, in the case of a phantom network. The network chains in the phantom model do not experience the effects of the surrounding chains and entanglements and, thus, move as "phantoms".[15,16] In eq. (7), ϕ is the junction functionality that represents the number of chains that meet at one junction.

The orientational behavior can be described by birefringence and by infrared dichroism. Birefringence is directly related to the second Legendre polynomial by the following expression:

$$\Delta n = [\Delta n]_0\,\langle P_2(cos\theta)\rangle. \qquad (8)$$

Both techniques are able to probe the orientational behavior of polymer chains at a molecular level, in contrast to the macroscopic information

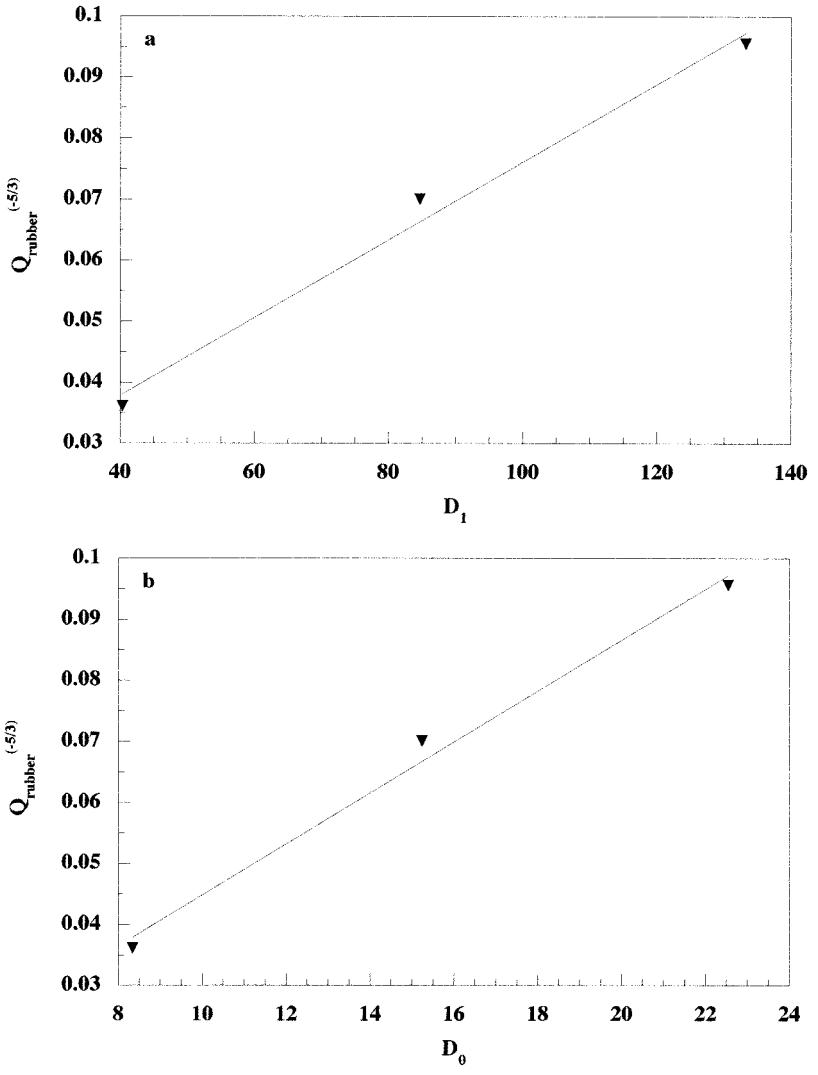

Figure 9 Correlation between swelling and orientational measurements. (a) Birefringence; (b) infrared dichroism.

provided by most other characterization techniques.

According to the theory, the birefringence is related to the strain function by the expression[21,22]

$$\Delta n = \frac{vkTC}{V}\mathcal{P}\,(\alpha^2 - \alpha^{-1}) = D_1\,(\alpha^2 - \alpha^{-1}), \quad (9)$$

where v/V represents the number of chains per unit volume, $\mathcal{P}$ is a factor equal to one for an affine network and $(1 - 2/\phi)$ for a phantom network, and C is the stress-optical coefficient that is related to the optical anisotropy Γ_2 of the network through the following equation:

$$C = \frac{2\pi\,(n^2 + 2)^2\,\Gamma_2}{27\,nkT}, \quad (10)$$

n being the mean refractive index. C is usually referred to in the literature as the stress-optical coefficient, as:

$$C = \Delta n/\sigma_t, \quad (11)$$

where σ_t is the true stress (force f divided by the deformed area A) given by

$$\sigma_t = \frac{vkT}{V}\,\mathcal{P}\,(\alpha^2 - \alpha^{-1}). \quad (12)$$

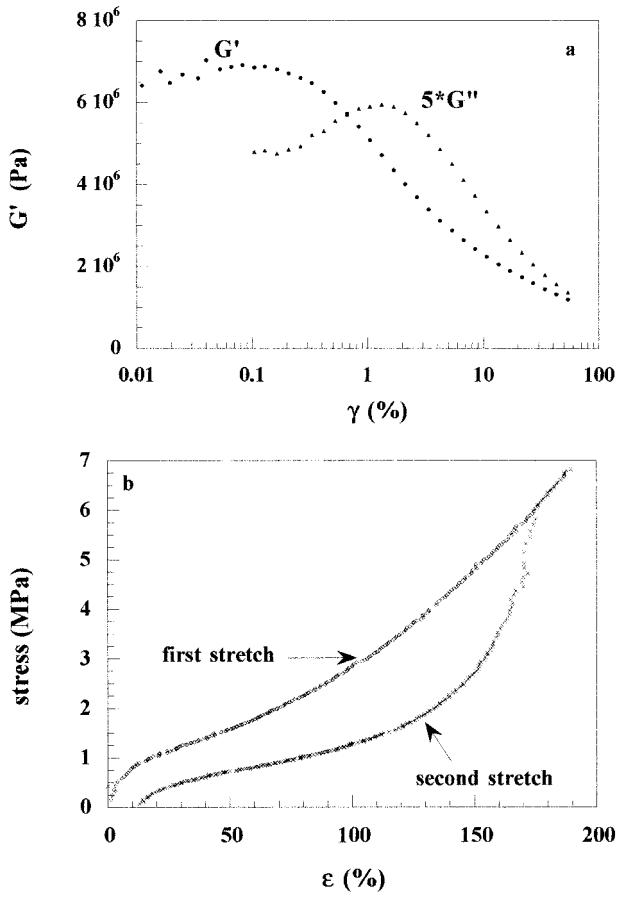

Figure 10 Energy dissipation phenomena. (a) Payne effect; (b) Mullins effect.

The absorption of infrared radiation is caused by the interaction of the electric field vector of the incident light with the electric dipole-transition moment associated with a particular molecular vibration.

The parameter commonly used to characterize the degree of optical anisotropy in stretched polymers is the dichroic ratio R, defined as $R = A_{//}/A_{\perp}$ ($A_{\parallel}$ and $A_{\perp}$ being the absorbances of the investigated band, measured with radiation polarized parallel and perpendicular to the stretching direction, respectively).[23–26]

The orientation function is related to the dichroic ratio R by this expression:

$$\langle P_2(\cos\,\theta)\rangle = \frac{2}{(3\cos^2\beta - 1)} \times \frac{(R-1)}{(R+2)}, \quad (13)$$

where β is the angle between the transition moment vector of the vibrational mode considered and the local chain axis of the polymer.

The theoretical models of rubber elasticity show that, in an affine network, the slopes of the strain dependences of the orientation function (D_0) and of the birefingence (D_1) vary as $1/M_c$. Both measurements are thus suitable to get an evaluation of the effective cross-linking density arising from the chemical junctions and also from the polymer–filler interaction. Thus, chain orientation is only sensitive to the total cross-linking density, contrary to the stress–strain measurements, which also contain the contribution arising from the inclusion of rigid particles. A comparison of the two sets of data will allows to quantify these two effects.

The midinfrared spectrum of the unfilled network is represented in Figure 3. On account of the strong intenity of the bands associated with the fundamental modes, we have examined the dichroic behavior of the band located at 2727 cm^{-1}. It is interesting that the band located at 837 cm^{-1} associated with the C–H out-of-plane bending mode of the *cis*-unit of the natural rubber macromolecular chains is shifted to higher wave numbers on stretching. This shift is attributed to the stress-induced crystallization of natural rubber[23] (Fig. 4). This phenomenon is responsible for the large increase in the stress observed at high deformation (Fig. 1) and can be better visualized by plotting the reduced stress σ^* [$\sigma^* = \sigma_t/(\alpha^2 - \alpha^{-1})$][27,28] against the reciprocal of the extension ratio α (Fig. 5) as suggested by the Mooney–Rivlin equation:

$$\sigma^* = 2C_1 + 2C_2\,\alpha^{-1}, \quad (14)$$

in which $2C_1$ and $2C_2$ are constants independent of α.

The large and abrupt increase in the reduced stress corresponds to a self-toughnening of the elastomer because the crystallites act as additional cross links in the network.

As seen in Figure 5, the samples filled with carbon black and silanized silica also display upturns in the reduced stress, attributed in this case to the limited chain extensibility of the short chains connectinf filler particles. Unfortunately, because of an overlap of the absorption bands of the silica and the elastomer, it was not possible to analyze the strain dependence of the C–H out-of-plane frequency, that would allow us to give a definitive answer on a possible crystallization process in filled systems.

Figure 6 shows the strain dependence of the birefringence and that of the dichroic function

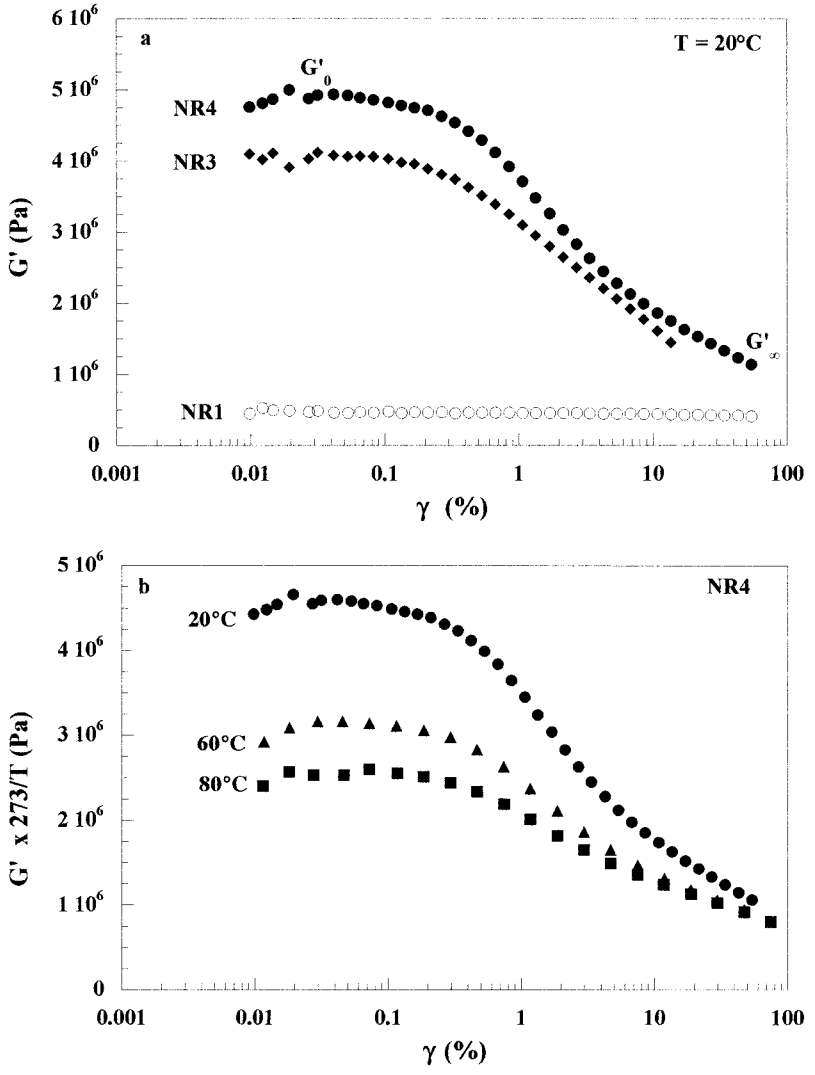

Figure 11 Effect of the nature of the interface (a) and of the temperature (b) on the Payne effect.

$(R-1)/(R+2)$ for the NR1, NR2, and NR3 samples. As expected, a large decrease in the orientation level, evidenced by birefringence and by infrared dichroism, is observed for the NR2 compound because of a decrease of the curing state caused by the presence of silica. This decrease in the cross-linking density reflected by an increase in the molecular weight between cross-links, M_c, can be easily determined from the orientational results.

The difference between the modulus of a filled elastomer and that of the unfilled network, at intermediate strains, may be regarded as to be a result of the product of two factors:

$$G = G_0 X Y,$$

where X arises from the inclusion of rigid particles in a nonrigid matrix, accounted for by the Guth and Gold expression. For a filler loading of 50 phr of silica, X is equal to 1.976. The second factor, Y, arises from filler–matrix linkages and can be accurately obtained from orientational measurements (from birefringence or infrared dichroism):

$$Y = [\Delta n_{\text{filled}}]/[\Delta n_{\text{unfilled}}] = [P_{2\,\text{filled}}]/[P_{2\,\text{unfilled}}] = [M_{c\,\text{unfilled}}/M_{c\,\text{filled}}].$$

By multiplying, at each given strain, the stress of the unfilled sample by the XY product leads, at

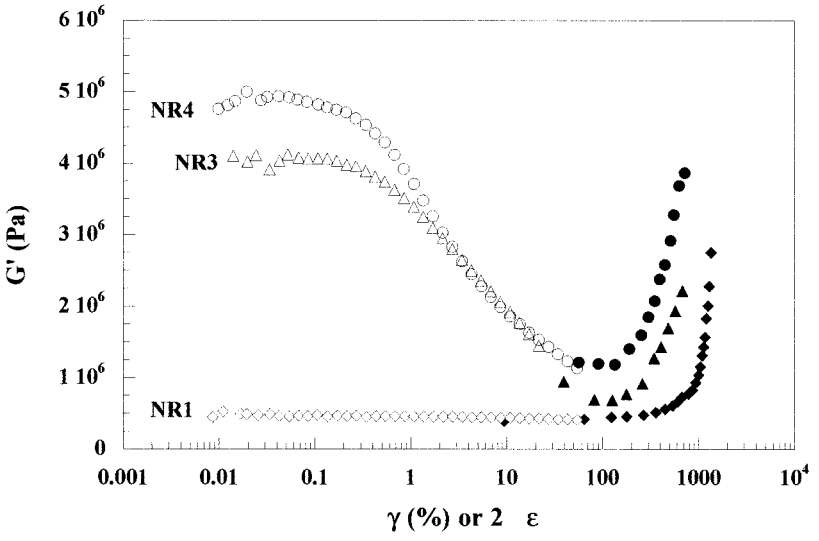

Figure 12 Correspondance between dynamic and tensile measurements. Filled labels = tensile data.

intermediate strains, to curves in acceptable agreement with the experimental ones (Fig. 7).

The D_1 and D_0 values, obtained from the slopes of the curves representing the birefringence, Δn or the dichroic function $(R - 1)/(R + 2)$ (Fig 6), can be nicely correlated, thus showing that both techniques reflect the total cross-linking density. Each coefficient can also be correlated with the apparent molecular weight between cross links (Fig. 8). It is also interesting to mention that at a high degree of swelling, Q (equal to V^1_{2m}), and under the assumption that the filler does not swell, a series expansion of eq. (3) leads to the following expresssion:

$$(1/M_c) \propto v_2^{5/3} = Q_{\text{rubber}}^{-5/3}. \quad (15)$$

$Q_{\text{rubber}}^{-5/3}$ can be correlated to D_0 and D_1, which are both proportional to I/M_c (Fig. 9).

Energy Dissipation Phenomena: Payne and Mullins Effects

Reinforced elastomers exhibit specific features that are related to energy dissipation phenomena. The first one, known as the Payne effect because it was studied extensively by Payne,[29,30] is generally demonstrated through the analysis of the low-strain dynamic properties of filled systems. It is observed at very small deformations and is characterized by a strong decrease in the storage modulus G′, associated with a maximum of the loss modulus G″ [Fig. 10(a)]. The second one, which is observed at high extensions, concerns the "Mullins effect" or "stress softening" and is characterized by a pronounced lowering in the stress when the filled vulcanizate is extended a second time [Fig. 10(b)].

Payne Effect. The dynamic behavior of filled rubbers is of great importance in the performance of rubber engineering components and is essential in tire applications.

The modulus drop $(\Delta G = G'_0 - G'_\infty)$ with strain amplitude, showing a typical nonlinear behavior, represents the Payne effect. At larger deformations, the difference between unfilled and filled rubber (G'_∞) contains the contribution arising from the inclusion of rigid particles (accounted for by the Guth and Gold expression) and also the contribution of the polymer–filler cross links to the network structure[31] [Fig. 11(a)]. The Payne effect is influenced by filler parameters: concentration, surface area, distribution, surface characteristics, and temperature.

As seen in Figure 11(a), the chemical modification of the silica particles by means of the coupling agent reduces the amplitude of the Payne effect (modulus drop with strain amplitude), the loss modulus, and tgδ, which is an important parameter in the rolling resistance of tires. Unfortunately, as a result of a poor curing reaction in 2-mm-thick samples, it was not possible to investigate the Payne effect in the NR2 sample. It already has been reported that nonmodified silica

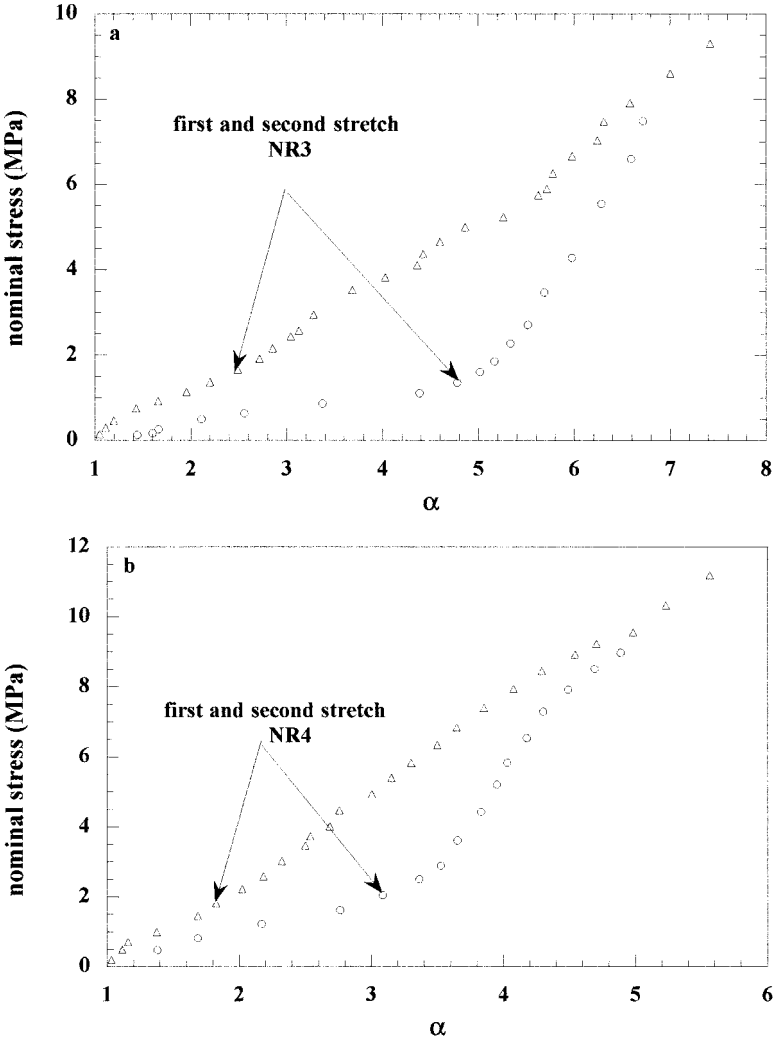

Figure 13 Mullins hysteresis displayed by the NR3 and NR4 samples.

leads to a much higher Payne effect than carbon black. In a hydrocarbon polymer, the polymer–silica interaction is low, and strong filler–filler interaction, via hydrogen bonding between silanol groups on the particle surface, leads to the formation of a filler network. The use of a coupling agent to enhance the degree of polymer–filler interaction minimizes filler networking and imparts improved performance properties to the filled materials.

In the past few years, many new ideas, theories and observations were reported on the dynamic properties of filled elastomers.[32–36] All of them highlight the importance of filler characteristics. Filler networking seems to be one of the main parameters that governs the dynamic stress–strain response. But the construction of the filler network can be achieved by different modes. First, by direct interparticle contacts, which is the case with a highly polar filler such as silica, or via a model of immobilized elastomeric layer where the particle surface is recovered with adhering elastomer molecules that extend into the continuous polymer phase. In the presence of filler–polymer interaction, the Payne effect is thus associated with a shell of hindered rubber at the particle surface and is the result of the displacement of the shell under the influence of applied stress. Within reasonable times, the displaced shell recovers its original undeformed state. In the case of strong polymer–filler interaction, a more tight shell is obtained, and this shell is resistant to mechanical deformation. This concept of the shell rubber, connected with physical adsorption of elastomer molecules, can also explain the strong decrease of the storage and loss moduli

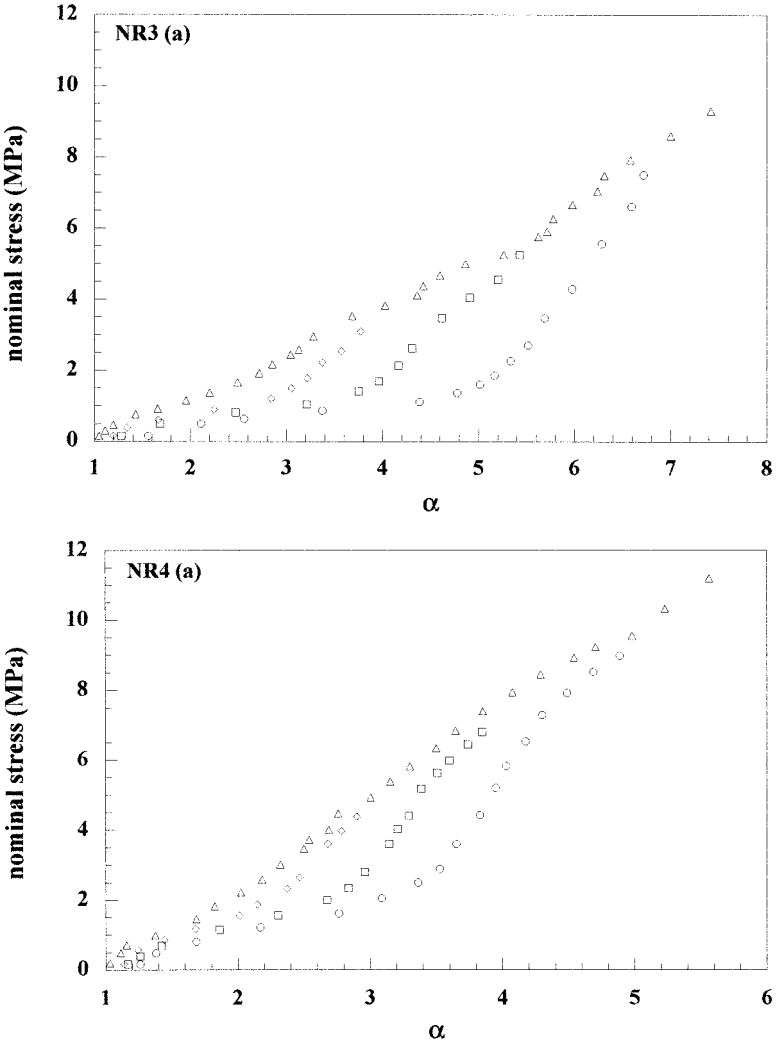

Figure 14 First and second stretching curves performed at various deformations at room temperature (a) and corresponding Mooney-Rivlin plots (b) for the NR3 and NR4 samples.

with increasing temperature [Fig. 11(b)]. The modulus values in Figure 11(b) have been corrected by the entropic factor T_{rcf}/T, where the reference temperature T_{rcf} has been chosen equal to 273 K.

Finally, despite the different modes of deformation (shear or elongation), it could be possible to correlate the low strain dynamic measurements to the first part of the tensile stress–strain curves. For that purpose, it is interesting to define the secant modulus as the true stress σ_t divided by the deformation ε:

$$E_{secant} = \sigma_t/\varepsilon. \quad (16)$$

According to the relation between the shear and elongation moduli $G = E / [2 (1 + v_p)]$ and to the value (0.5) of the Poisson coefficient for an elastomeric material,

$$G = E_{secant}/3.$$

The tensile data represented in Figure 12 as E_{secant} versus $\gamma = 2\varepsilon$ describe the end of the Payne effect; they pass through a minimum then increase sharply because of the limited chain extensibility (Fig. 12).

Mullins Effect. Also related to an energy dissipation phenomenon is the Mullins effect, or stress softening effect, observed at high extensions and characterized by a pronounced lowering in the stress when the filled vulcanizate is extended the

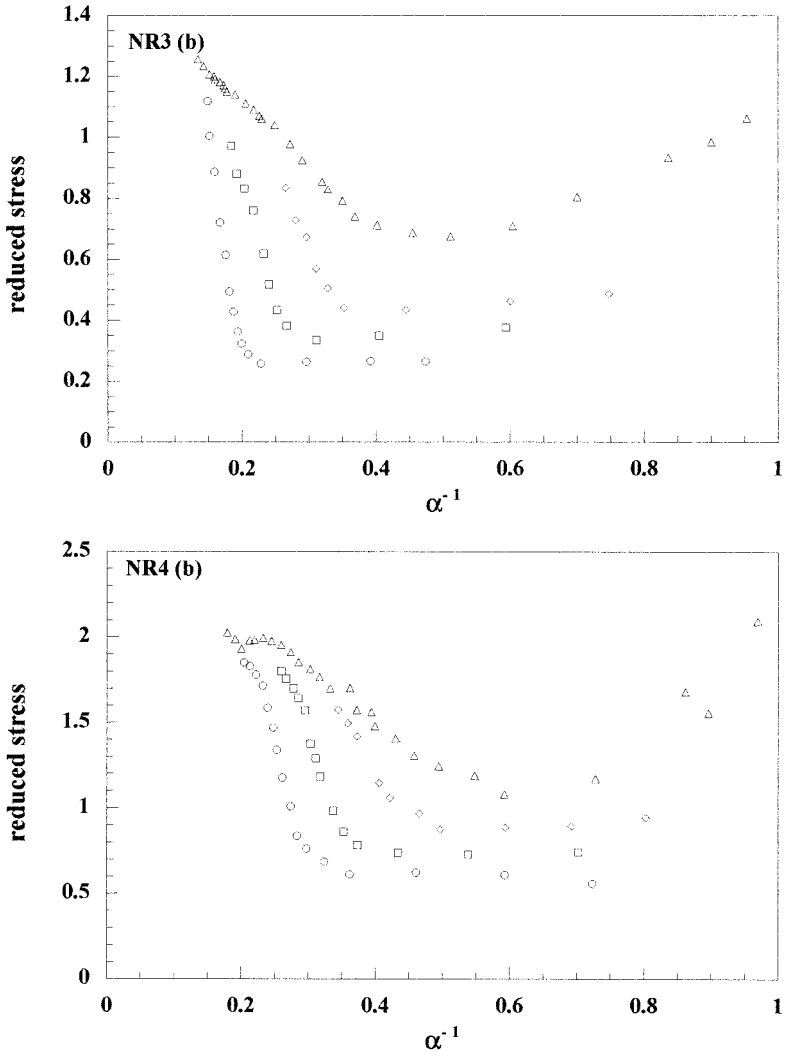

Figure 14 (*Continued from the previous page*)

second time [Fig. 10(b)]. Unfilled rubbers display much less stress softening. Fillers cause stress softening at lower bulk strains than do unfilled rubbers. This phenomenon has been the subject of much study and controversy, and several mathematical treatments have been proposed on the basis of a combination of rupture mechanisms. In their phenomenological theory for this effect, Mullins and Tobin[37] considered the filled rubber to be composed of hard and soft regions, a fraction of hard regions becoming soft after a prestretching of the sample. The authors suggested that a breaking up of the filler aggregates or of polymer–filler bonds might be involved in this process. In a later work, Blanchard and Parkinson[38,39] presented a quantitative description in which they concluded that the stress-softening effect was result of the breakage of weak polymer–filler linkages. The molecular model proposed by Bueche[40] is based on the concept of the breakage of chains of different lengths extending between adjacent filler. Shorter chains will rupture first and will not contribute to the modulus on the second stretch. Longer chains will break at higher deformations applied to the sample. The work of Bueche was intended to relate softening behavior to molecular parameters in the rubber and, essentially, to the length of a statistical segment, the area per site, the tension in the chain at break, and the average surface separation to the influence of the reinforcing filler. Dannenberg[41] proposed a model for stress softening that included slippage of the elastomer chains at the filler surface, leading to a stress redistribution to neigh-

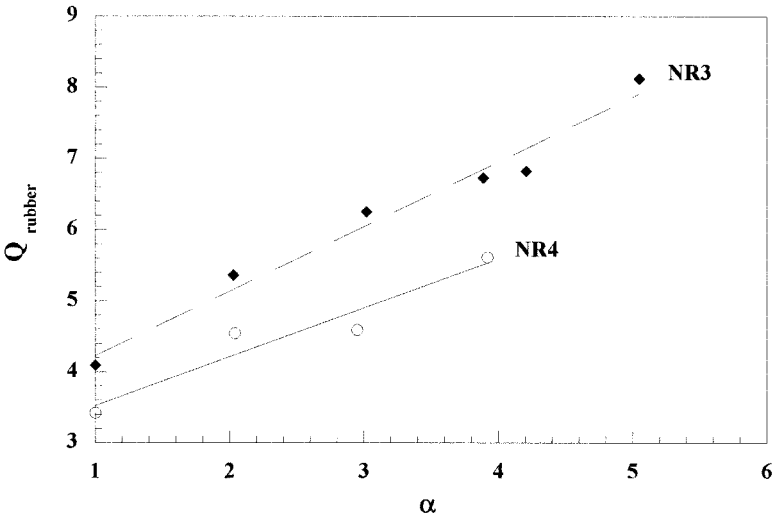

Figure 15 Dependence of the equilibrium swelling ratio of the rubber on the strain value applied on prestretching of the samples.

boring molecules. In each model, the softening effect is attributed to a decrease in the number of elastically effective network chains, which is proportional to the stress. As it will be seen below, the network chains broken during extension of filled rubbers with high strains can be demonstrated by equilibrium-swelling measurements.

The Mullins hysteresis (area between the first and the second stretch) obtained when natural rubber is filled with carbon black and with silica used with the coupling agent is reported in Figure 13.

First and second stretchings performed at different strain values, as well as the corresponding Mooney–Rivlin representations, are illustated in Figure 14 for the NR3 and NR4 samples. It is worth noting that the limited chain extensibility of the network chains occurs at higher strains for the second stretchings and at increasing strain values for second extensions performed at increasing strain.

From the above observations, it seems reasonable to deduce that the stress-softening effect corresponds to the breakage or the slippage of chains having reached their limited extensibility. This interpretation is confirmed by equilibrium solvent swelling after prestretching of the filled samples (Fig. 15).

CONCLUSION

This article reports recent investigations performed on filled natural rubber. It shows that a better insight into the reinforcement mechanisms is obtained by combining different experimental techniques. Molecular measurements of chain orientation are nicely combined with mechanical data, which allows a deeper understanding of the reinforcement fundamentals.

REFERENCES

1. Kraus, G. Reinforcement of Elastomers; Wiley: New York, 1965.
2. Dannenberg, E. M. Rubber Chem Technol 1975, 48, 410.
3. Wagner, M. P. Rubber Chemistry and Technology, 1976, 49, 703.
4. Voet, A. J Polym Sci: Macromol Rev 1980, 15, 327.
5. Edwards, D. C. J Mater Sci 1990, 25, 4175.
6. Ahmed, S.; Jones, F. R. J Mater Sci 1990, 25, 4933.
7. Wolff, S. Rubber Chemistry and Technology, 1996, 69, 325.
8. Goerl, U.; Hunsche, A.; Mueller, A.; Koban, H. G. Rubber Chemistry and Technology, 1997, 70, 608.
9. Hashim, A. S.; Azahari, B.; Ikeda, Y.; Kohjiya, S. Rubber Chemistry and Technology 1998, 71, 289.
10. Bokobza, L. Poly Int 2000, 49, 743.
11. Kralevich, M. L.; and Koenig, J. L. Rubber Chem Technology 1998, 71, 300.
12. Guth, E.; Gold, O. Phys Rev 1938, 53, 322.
13. Guth, E. J Appl Phys 1945, 16, 20.
14. Einstein, A. Ann Physik (Leipzig) 1906, 19, 289.
15. Mark, J. E.; Erman, B. Rubber Elasticity. A molecular Primer, Wiley-Interscience: New York, 1988.
16. Erman, B.; Mark, J. E. Structure and Properties of Rubberlike Networks, Oxford University Press: New York, 1997.

17. Jasse, B.; Koenig, J. L.; J Macromol Sci Rev Macromol Chem, 1979, C17, 61.
18. Roe, R. J.; Krigbaum, W. R.; J Appl Phys 1964, 35, 2215.
19. Erman, B.; Haliloglu, T.; Bahar, I.; Mark, J. E.; Macromolecules 1991, 24, 901.
20. Besbes, S.; Cermelli, I.; Bokobza, L.; Monnerie, L.; Bahar, I.; Erman, B.; Herz, J. Macromolecules 1992, 25, 1949.
21. Erman, B.; Flory P. J. Macromolecules 1983, 16, 1601.
22. Erman, B.; Flory, P. J. Macromolecules 1983, 16, 1607.
23. Amram, B.; Bokobza, L.; Queslel, J. P.; Monnerie, L. Polymer 1986, 27, 877.
24. Amram, B.; Bokobza, L.; Monnerie, L.; Queslel, J. P. Polymer 1988, 29, 1155.
25. Bokobza, L.; Amram, B.; Monnerie, L.; In Elastomeric Polymer Networks: Ed. Mark, E.; Erman, B. Prentice Hall: Englewood Cliffs, New Jersey, 1992; p. 289.
26. Bokobza, L.; Macron, C. The Wiley Polymer Networks Group Series; Stokke, B. T.; Elgsaeter, A. Ed.; Wiley: New York, 1999; Vol. 2, p. 199.
27. Mooney, M. J App Phys 1948, 19, 434.
28. Rivlin, R. S. Phil. Trans Rubber So Lond A 1948, 241, 379.
29. Payne, A. R. J Polym Sci 1962, 6, 57.
30. Payne, A. R.; Whittaker, R. E. Rubber Chem Technol. 1971, 44, 440.
31. Payne, A. R. In Reinforcement of Elastomers; Kraus, G, Ed.; Interscience Publishers: New York, 1965; Chapter 3.
32. Kraus, G. J Appl Polym Sci. Appl Polym Symp. 1984, 39, 75.
33. Ulmer, J. D. Rubber Chem Technol 1996, 69, 15.
34. Maier, P. G.; Göritz, D. Kautschuk Gummi Kunststoffe 1996, 49, 18.
35. Wang, M.-J. Rubber Chem Technol 1998, 71; 520; 1999, 72, 430.
36. Göritz, D.; Raab, H.; Frölich, J.; Maier, P. G. Rubber Chem Technol 1999, 72, 929.
37. Mullins, L.; Tobin, N. R. Rubber Chem Technol 1957, 30, 555.
38. Blanchard, A. F.; Parkinson, D. Ind Eng Chem 1952, 44, 799.
39. Blanchard, A. F. J Polymer Sci. 1954, 14, 355.
40. Bueche, F. J Appl Polym Sci 1960, 4, 107.
41. Dannenberg, E. M. Trans Inst Rubber Ind. 1966, 42, T26.